Published in final edited form as:
Dev Cell. 2009 September ; 17(3): 377–386. doi:10.1016/j.devcel.2009.07.011.

Local Guidance of Emerging Vessel Sprouts Requires Soluble Flt-1 (VEGFR-1)

John C Chappell[1,2], **Sarah M Taylor**[1,2], **Napoleone Ferrara**[4], and **Victoria L Bautch**[1,2,3,5]

[1]Dept. of Biology, The University of North Carolina at Chapel Hill, Chapel Hill, NC, 27599, USA

[2]Carolina Cardiovascular Biology Center, The University of North Carolina at Chapel Hill, Chapel Hill, NC, 27599, USA

[3]Lineberger Comprehensive Cancer Center, The University of North Carolina at Chapel Hill, Chapel Hill, NC, 27599, USA

[4]Genentech, Inc., South San Francisco, CA, 94080, USA

Summary

Blood vessel networks form via sprouting of endothelial cells from parent vessels. Extrinsic cues guide sprouts once they leave the initiation site, but these cues are likely insufficient to regulate initial outward movement, and many embryonic vessel networks form in the absence of a strong extrinsic gradient. We hypothesized that nascent sprouts are guided by spatial cues produced along their own vessels, and that soluble Flt-1 (sFlt-1) participates in this guidance. Analysis of developing vessels with perturbed *flt-1* function revealed mis-guided emerging sprouts, and transgenic sFlt-1 rescued sprout guidance parameters. sFlt-1 activity in endothelial cells immediately adjacent to the emerging sprout significantly improved local sprout guidance. Thus we propose that a vessel-intrinsic system initially guides emerging sprouts away from the parent vessel, utilizing spatially regulated expression of sFlt-1 in conjunction with exogenous VEGF. Local sprout guidance defects are predicted to contribute to vessel dysmorphogenesis during perturbed development and disease.

Keywords

vessel branching; VEGF; soluble Flt-1; sprout guidance; angiogenesis; ES cells; retinal vessels

Introduction

Blood vessel networks are required to provide oxygen and nutrients to developing embryos, and they also promote tumor growth and metastasis (Risau, 1997). Vascular networks form and expand via sprouting angiogenesis, a process whereby endothelial cells form a sprout that migrates away from the parent vessel, and eventually connects with another vessel or sprout (Horowitz and Simons, 2008; Lu and Werb, 2008). Vascular patterning cues extrinsic to developing vessels are important in vessel network formation. Angiogenic factor gradients are

5Corresponding author: Victoria L Bautch, PhD, Dept of Biology, CB#3280, The University of North Carolina at Chapel Hill, Chapel Hill, NC 27599, phone 919-966-6797, Fax 919-962-8472, bautch@med.unc.edu.

The authors declare no conflict of interest.

produced by tumor cells and embryonic structures, such as the brain, and these cues guide the overall direction of vessel migration and plexus formation by essentially "pulling" the vessels in appropriate directions. However, these extrinsic signals are likely not the only important guidance cues, because vascular networks often form in the absence of a strong extrinsic gradient (Czirok et al., 2008). For example, embryonic stem cells differentiate into multiple cell types in culture, and vessel networks form above a layer of signal-producing endoderm that instigates vessel formation but does not provide obvious patterning cues (Kearney and Bautch, 2003; Keller, 2005). This process mimics vessel development in the embryonic yolk sac, where the vasculature expands over rather than into the signal-producing endoderm (Damert et al., 2002). Moreover, emerging sprouts normally never interact with the parent vessel or nearby sprouts, suggesting that specific cues guide the initial outward migration of a vascular sprout. However, local sprout guidance cues have not been described.

The extrinsic cues that guide vessel network patterning are provided by several signaling pathways, including VEGF, BMP/TGFβ, and Wnt (Eichmann et al., 2005; Holderfield and Hughes, 2008). Among these, the role of VEGF-A signaling in vessel morphogenesis is best understood (Coultas et al., 2005; Kowanetz and Ferrara, 2006; Li et al., 2008; Gerhardt, 2008). VEGF-A is secreted by target tissues or tumors, and distinct isoforms generated by alternative splicing have differential affinity for heparin, and presumably for extracellular matrix. VEGF120 is proposed to diffuse freely, while VEGF164 binds moderately and VEGF188 more strongly to the matrix, thus producing a VEGF-A gradient from the source that provides extrinsic guidance by "pulling" the nascent vessel towards the higher ligand concentration. VEGF-A interacts with two high-affinity tyrosine kinase receptors on endothelial cells, Flk-1 (VEGFR-2) and Flt-1 (VEGFR-1). The importance of this pathway is underscored by the embryonic lethality with vascular defects that results from genetic deletion of any of these genes (Carmeliet et al., 1996; Ferrara et al., 1996; Fong et al., 1995; Shalaby et al., 1995). Mice expressing individual VEGF-A isoforms have aberrant vessel morphogenesis (Ruhrberg et al., 2002; Stalmans et al., 2002), but in all cases vessel sprouting and network formation occur, suggesting that a VEGF-A gradient is not essential to the formation of vessel networks.

VEGF-A signaling through Flk-1 is well-understood, and endothelial cell proliferation, migration, and survival are promoted via downstream signal transduction pathways. In contrast, the role of Flt-1 is less understood. Genetic loss of *flt-1* leads to vessel dysmorphogenesis and overgrowth (Fong et al., 1995; Kearney et al., 2002). Flt-1 is alternatively spliced to produce both a membrane-localized form (mFlt-1) and a soluble form (sFlt-1) that is secreted from endothelial cells, and sFlt-1 can act as a ligand sink to modulate the amount of VEGF-A available for Flk-1 binding (Kendall and Thomas, 1993; Roberts et al., 2004). We previously showed that Flt-1 negatively regulates endothelial cell proliferation, but it positively modulates the rate of sprout initiation and migration (Kearney et al., 2002; Kearney et al., 2004). These functions result from the differential effects of the Flt-1 isoforms on endothelial proliferation vs. branching morphogenesis, as endothelial expression of sFlt-1 but not mFlt-1 rescued branching (Kappas et al., 2008).

Here we identify a form of sprout guidance that acts in the local vicinity of the emerging vessel sprout, and is required to efficiently guide newly formed sprouts away from the parent vessel. This local sprout guidance contributes to vessel network patterning. We show that local sprout guidance requires sFlt-1 activity in cells adjacent to the sprout, and provide a mechanistic model for the effects of sFlt-1 on vessel morphogenesis. We propose that secreted sFlt-1 precisely inactivates VEGF-A on either side of the sprout to provide a ligand corridor for the emerging sprout, and this cue effectively "pushes" the sprout in the proper direction.

Results

sFlt-1 is required for local sprout guidance

Because emerging blood vessel sprouts normally move away from the initiation site and do not join with the parent vessel or nearby sprouts, we hypothesized that local guidance cues exist to ensure this directed migration and properly expand the vessel network. We further hypothesized that vessel-produced sFlt-1 was required to locally integrate information provided by extrinsic VEGF, because soluble Flt-1 (sFlt-1) is produced by developing vessels and affects branching morphogenesis, and extrinsic VEGF-A affects sprouting behavior (Kearney et al, 2004; Kappas et al, 2008). To test these hypotheses, we first utilized a model of vessel development whereby mouse embryonic stem (ES) cells differentiate in vitro to form a lumenized vessel network, in the context of other embryonic cell types that provide initial patterning cues (Jakobsson et al., 2007; Kearney and Bautch, 2003). Although ES cell-derived vessels are not exposed to blood flow, they recapitulate early vessel network formation in vascular beds such as the yolk sac, which forms prior to the onset of flow (Larina et al, 2009). Moreover, most sprouting angiogenesis occurs in situations of absent or low blood flow. Visual inspection of ES-derived vessel sprouts indicated that WT sprouts in general had angles between 50°-90° relative to the parent vessel, and were 75 μm or greater from another vessel structure. In contrast, sprouts from vessels lacking Flt-1 (*flt-1*$^{-/-}$) had more acute angles relative to the parent vessel, and formed closer to other vessels or sprouts, and quantification of these parameters confirmed our observations (Fig. 1 A-B, E-F, Supp. Fig. 1). We reasoned that sprout direction was regulated by tip cell filopodia, and that these sensors might be perturbed in *flt-1* mutant vessels. Indeed, the angle of sprout filopodia relative to the sprout axis was predominately within 60° (of a 180° arc) for WT sprouts but randomized in *flt-1*$^{-/-}$ mutant sprouts (Fig. 1G). We next determined the relative contributions of the two Flt-1 isoforms, utilizing *flt-1* mutant ES cell lines that were selectively rescued for either sFlt-1 (soluble) or mFlt-1 (membrane-anchored) via endothelial cell-expressed transgenes (Kappas et al., 2008). sFlt-1 expressing vessels had sprouts similar to WT sprouts – they emerged at angles close to 90° from the parent vessel and away from other sprouts, and their filopodia followed the sprout axis (Fig. 1C). All parameters of local sprout guidance in sFlt-rescued vessels were similar to WT and significantly different from mutant sprouts (Fig. 1, E-G). In contrast, vessels expressing mFlt-1 resembled mutant sprouts and were significantly different from WT sprouts in all parameters of local sprout guidance (Fig. 1D, E-G).

To determine whether the pattern of fixed sprouts reflected sprout emergence patterns, we next used live image analysis. WT or *flt-1*$^{-/-}$ mutant ES cells transgenic for PECAM-eGFP (Kearney et al., 2004) were imaged. Visual inspection indicated that WT sprouts emerged at an angle close to 90° from the parent vessel, and they tended to stay on the original sprout axis and move forward efficiently (Fig. 2A, Supp. Movie S1). In contrast, *flt-1* mutant sprouts often emerged at acute angles, and they changed the angle frequently, so overall they had less forward motion than WT sprouts (Fig. 2B, Supp. Movie S2). Mutant sprouts also curled back, and sometimes they joined the parent vessel. Quantification of the average sprout angle and average rate of angle change over time showed that these parameters were significantly different between WT and *flt-1* mutant sprouts (Fig. 2, C-D).

To further determine whether local sprout guidance required a ligand gradient, we analyzed sprout emergence as a result of exogenous VEGF165 stimulation in a embryoid body collagen model (Jakobsson et al., 2007). Once vessel sprouts emerged from the embryoid body, they continued to branch and form secondary sprouts (Supp Fig. 2). These secondary sprouts differed between WT and *flt-1* mutant vessels, and mutant sprouts formed at more acute angles to the parent vessel (Supp Fig. 2, A-B, E-F). Embryoid bodies expressing only sFlt-1 had secondary sprout angles that appeared similar to WT angles, and those expressing only mFlt-1 had secondary sprout angles that appeared closer to *flt-1* mutant angles (Supp Fig. 2 C-D, G-

H). Quantification showed significant differences between WT and *flt-1* mutant sprouts, and sprout angles in sFlt-1 but not mFlt-1 expressing vessels were rescued (Supp. Fig. 2I). Taken together, these data show that soluble Flt-1 is required for local sprout guidance, and that local guidance is operative even when no obvious ligand gradient is present.

Loss of *flt-1* function and ectopic VEGF-A perturb local sprout guidance of retinal vessels

To determine if local sprout guidance is relevant in vivo, we examined vessel sprouts that formed in the early post-natal retina, since development of this vascular network is well-characterized, and retinal vessels express Flt-1 (Fruttiger, 2002). Untreated vessels had well-spaced sprouts with few bifurcations (Fig. 3A, C-D). Prominent filopodia are a hallmark of retinal endothelial cells, especially on the tip cells at the leading edge of each sprout (Gerhardt et al., 2003). Thus we analyzed both the number of filopodia and the angle of the filopodia relative to the sprout axis, and found that filopodia angles showed a similar distribution to WT sprouts of ES cell-derived vessels (Fig. 3, E-F). These data suggest that local sprout guidance is involved in proper retinal vascular development.

To determine whether excess ligand could perturb local sprout guidance, we examined retinas that were exposed to exogenous VEGF-A (Fig. 3B). Visual examination showed that VEGF-exposed sprouts formed closer to each other and had more bifurcations than PBS-treated controls, indicating that these parameters of local sprout guidance were perturbed, and quantification confirmed these observations (Fig. 3B, C-D). The presence of numerous bifurcated sprouts suggested that the filopodia angles were randomized in retinal vessels exposed to ectopic VEGF-A. Both visual examination and quantification confirmed that filopodia numbers were significantly increased, and filopodia angles were randomized compared to controls (Fig. 3B, E-F).

To further test the role of Flt-1 in local sprout guidance in vivo, we perturbed *flt-1* function in developing retinas using two strategies (Fig. 4). We neutralized Flt-1 by injecting a neutralizing (ligand-binding) antibody, and found that sprout bifurcations and filopodia numbers were significantly increased, while filopodia angles relative to the sprout axis were significantly randomized in the antibody-injected retinas (Fig. 4A-F). Distances between sprouts were not significantly affected by treatment with the flt-1 neutralizing antibody. This may reflect that sprout distances are a more long-term readout of sprout guidance than bifurcations or changes in filopodia, and the treatment window was for 6 hours. We next utilized a genetic approach to reduce *flt-1* function in the developing retina, by exposing developing retinas of *flt-1*$^{flox/flox}$ mice to adenovirus-expressing Cre recombinase (Ad-Cre) (Fig. 4G-L). Exposure of retinal vessels to Ad-Cre, but not Ad-GFP, increased the proximity of sprouts to other sprouts and increased the number of sprouts with bifurcations, although these were trends and not statistically significant. The lack of significance to these parameters may result from mosaic excision of *flt-1*. However, the filopodia angle was significantly randomized relative to the sprout axis in Cre-exposed retinas, and the number of filopodia was also significantly increased in the *flt-1*$^{flox/flox}$ retinas exposed to Cre recombinase (Fig. 4K-L). Thus local sprout guidance in retinal vessels is sensitive to perturbations of VEGF signaling and loss of *flt-1* function.

sFlt-1 expression in lateral base areas rescues local sprout guidance

To examine the hypothesis that soluble Flt-1 provides a negative cue important for local vessel sprout guidance, we analyzed the spatial expression and requirement for Flt-1 in emerging sprouts of ES cell-derived vessels and retinal vessels in vivo. We utilized the β-galactosidase reporter linked to the *flt-1* locus to examine expression in *flt-1*$^{+/-}$ and *flt-1*$^{-/-}$ES cell-derived vessels, and in *flt-1*$^{+/-}$ retinal vessels (Fig. 5). Visual inspection indicated that endothelial cells in the sprout proper had reduced levels of β-galactosidase expression relative to cells immediately adjacent to the sprout on each side, in locations we call sprout lateral base areas

(Fig. 5A-D, E-H, M-P). Quantitative analysis showed that average ratios of sprout to base area β-galactosidase reactivity were significantly less than 1.0 in both ES cell-derived vessels and retinal vessels (Fig. 5U). Flt-1 protein reactivity was also reduced in the sprout proper relative to the lateral base areas in WT ES-derived and retinal vessels (Fig. 5I-L, Q-T). Together these data suggest that Flt-1 expression is elevated in cells immediately adjacent to sprouts.

To determine the spatial requirements for *flt-1* function, we generated mosaic vessels by mixing WT ES cells with *flt-1*$^{-/-}$ ES cells prior to differentiation (Fig. 6). Using expression of β-galactosidase from the *flt-1* locus to identify mutant endothelial cells in mosaic vessels, we investigated sprouts that were WT but had mutant cells immediately adjacent to the sprout in the lateral base areas. These mosaic sprouts had a mutant phenotype even though the sprout proper was WT (Fig. 6A-D), and quantification of local sprout guidance parameters showed that these mosaic sprouts had mutant values (WT vs. WT:*flt-1*$^{-/-}$, sprout angle $p \leq 0.003$, sprout distance $p \leq 1 \times 10^{-7}$, filopodia angle, $p \leq 1 \times 10^{-8}$; *flt-1*$^{-/-}$vs. WT;*flt-1*$^{-/-}$, sprout angle $p \leq 0.9$, sprout distance $p \leq 1.0$, filopodia angle $p \leq 0.2$). Mosaic sprouts of the opposite structure, with a mutant sprout proper and WT lateral base area, appeared more WT, but since mutant sprouts had more variation in guidance parameters these data were not significant (data not shown). Thus the genotype of the lateral base areas for *flt-1* determines the phenotype of the emerging sprout, and the genotype of the sprout proper does not appear to be relevant for the sprout guidance phenotype.

We then generated mosaic vessels that were a combination of WT and *flt-1*$^{-/-}$;PECAM-sFlt-1 or *flt-1*$^{-/-}$;PECAM-mFlt-1 endothelial cells, to determine which Flt-1 isoform was required in the sprout lateral base areas. Mosaic sprouts that were WT with a lateral base area expressing sFlt-1 appeared WT (Fig. 6E-H), and quantification showed that sprout angle and filopodia angles were significantly rescued by the sFlt-1 transgene, while distance to the next vessel was similar to WT values (Fig. 6M-O). In contrast, similar analysis of mosaic sprouts that were WT with a lateral base area expressing mFlt-1 indicated that sprout guidance was not rescued (Fig. 6I-L), and quantification showed that all sprout guidance parameters retained mutant values (Fig. 6M-O). Moreover, comparison of mosaic sprouts that were identical except for expression of either sFlt-1 or mFlt-1 in lateral base areas showed that sprout angle and filopodia angle were significantly different from each other (sprout angle, $p \leq 0.04$, filopodia angle, $p \leq 1 \times 10^{-7}$). Thus expression of sFlt-1, but not mFlt-1, specifically in the lateral base areas of emerging sprouts, rescues local sprout mis-guidance that results from loss of *flt-1* in these areas.

Discussion

The work described here reveals a novel guidance system that locally regulates sprouting morphogenesis during blood vessel formation. This system provides the emerging sprout with local vessel-derived guidance cues that integrate with extrinsic cues to “push” sprouts away from the parent vessel. Local sprout guidance requires sFlt-1 in vessel areas immediately adjacent to the sprout, and we propose that secreted sFlt-1 precisely inactivates VEGF-A in these areas, leaving a ligand corridor that guides the emerging sprout (Fig. 7). This guidance is required for sprouts to efficiently leave the initiation site and move outward, and eventually fuse with other sprouts or vessels.

The existence of a local sprout guidance system explains how a vessel network can form and expand in the absence of a strong vector in extrinsic cues, such as is thought to occur in vascular development in the yolk sac and the embryonic head plexus (Damert et al., 2002). The parameters measured here, including the angle of the sprout relative to the parent vessel and the distance of the sprout to the nearest sprout or vessel, showed that WT sprouts generally emerge and move forward at approximately right angles relative to the parent vessel, and at distances from another vessel structure that minimize premature interactions. Dynamic image

analysis corroborated these data and showed that WT sprouts kept "on track" with minimal angle change over time. In contrast, *flt-1* mutant sprouts had randomized angles relative to the parent vessel, with many more sprouts emerging at acute angles and close to other structures. Filopodia are the endothelial sensors for sprouting migration found predominately on the tip cell of a sprout, and filopodia aligned with the sprout axis in controls but were randomized in *flt-1* mutant sprouts. Dynamic image analysis confirmed that loss of *flt-1* results in locally misguided sprouts with less stable trajectories. Moreover, mutant sprouts curled back and fused with the parent vessel on occasion, suggesting how dilated and unbranched vessels might form as a result of perturbed local sprout guidance.

Local sprout guidance was also relevant to proper vessel patterning in the developing retina. Several extrinsic guidance cues for retinal vessel patterning are known, including VEGF-A that forms an increasing gradient in distal regions, and an astrocyte template that patterns vessels (Fruttiger, 2002). However, the astrocyte template is more complex than the vessel sprouting pattern (Dorrell et al., 2002), so sprouts have multiple choices for forward motion. Vessel sprouts exposed to high levels of VEGF-A formed closer to adjacent sprouts and had a high frequency of bifurcations and randomized filopodia angles, indicating that local sprout guidance was perturbed. Although ectopic VEGF perturbs extrinsic vessel patterning cues (Gerhardt et al., 2003), these findings suggest that excess VEGF also overwhelmed *flt-1* regulation of local sprout guidance in the retinas. This conclusion was further corroborated by the finding that some local sprout guidance parameters were also perturbed in retinas that experienced loss of *flt-1* function, either through neutralization or via Cre-mediated excision. These findings suggest that the VEGF gradient provides insufficient information for sprout guidance in the immediate vicinity of the parent vessel, and that additional cues imparted by vessel-derived Flt-1 are required for proper local sprout guidance.

The retinal data highlights that local sprout guidance operates via interactions between extrinsic VEGF and vessel-derived Flt-1, but what is the mechanism whereby Flt-1 contributes to this process? Analysis of *flt-1* mutant sprouts expressing transgenic sFlt-1 or mFlt-1 showed that only sFlt-1 was capable of rescuing local sprout guidance parameters. Since sFlt-1 is made and secreted by endothelial cells, this indicated that local sprout guidance requires vessel-intrinsic signals, but it did not distinguish cell autonomous from non-cell autonomous effects. However, mosaic analysis clearly showed that the genotype of the sprout does not determine if sprouts are locally guided, since WT sprouts in a mutant context behaved like *flt-1* mutant sprouts. Instead, sFlt-1 activity is required in the cells immediately adjacent to the sprout, called the lateral base area. This leads to a proposed model (Fig. 7) in which initial sFlt-1 expression discontinuities are amplified, so that lateral base areas express and secrete sFlt-1. This localized sFlt-1 expression neutralizes the VEGF gradient immediately ahead of these areas but leaves a corridor directly in front of the emerging sprout with intact VEGF. The sprout senses VEGF via filopodia, and directs its initial forward motion straight ahead because this is the area of highest effective VEGF in the vicinity. This model predicts that expression of sFlt-1 is higher in the lateral base areas, in order to set up the zone of VEGF neutralization, and both β-galactosidase expression from the *flt-1* locus and Flt-1 protein expression showed some enrichment in the lateral base areas relative to the sprout proper. Thus a vessel-intrinsic local sprout guidance system utilizing sFlt-1 may intersect with extrinsic VEGF to "push" the emerging sprout away from the parent vessel. It is not clear how information is communicated locally to set up these spatial domains. However, the Notch-Delta pathway is a prime candidate to be involved in the cell-cell communication required to set up expression domains, since it intersects with VEGF signaling, and it is involved in setting up other local domains, such as tip cells vs. stalk cells, within the sprout (Gridley, 2007; Hellstrom et al., 2007;Holderfield and Hughes, 2008;Roca and Adams, 2007;Shawber et al., 2007;Suchting et al., 2007).

What is the physiological and pathological significance of a vessel-intrinsic local guidance system? It implies that the earliest events of sprouting have a distinct guidance regulation that differs from later events, when sprouts actively probe their environment for fusion partners. Local sprout guidance utilizes extrinsic cues such as VEGF, but it exhibits a distinct genetic requirement for vessel-derived sFlt-1. Perturbations of local sprout guidance likely contribute to vessel dysmorphogenesis in disease. For example, the dilated vessels that are hallmarks of tumors may result in part from sprout collapse into the parent vessel, and a recent paper showed that abnormal tumor vessels had reduced levels of sFlt-1 relative to tumor vessels "normalized" by changes in oxygen sensing (Mazzone et al, 2009). Local sprout guidance may also contribute to the disorganized vascular tumors called hemangiomas, since they also exhibit reduced Flt-1 expression (Jinnin et al., 2008). Finally, the sophistication and complexity of sprout guidance mechanisms emphasizes that therapeutic interventions to produce new blood vessels *in situ* will require extensive knowledge of the elegant controls that normally regulate vessel network formation.

Experimental Procedures

Cell Culture and In Vitro Differentiation

Maintenance and differentiation of ES cells was as described (Kearney and Bautch, 2003): WT, *flt-1*$^{-/-}$ (gift of G.H. Fong), and *flt-1*$^{-/-}$ containing an sFlt-1 or mFlt-1 transgene linked to the PECAM promoter-enhancer in the ROSA26 locus (Kappas et al., 2008). Hanging drop differentiation was used to generate EBs for mosaic vessel formation as described (Kearney et al, 2003), by combining WT ES cells in a 1:1 ratio with either *flt-1*$^{-/-}$, *flt-1*$^{-/-}$; PECAM-sFlt-1, or *flt-1*$^{-/-}$; PECAM-mFlt-1 ES cells.

Intraocular Injections

Intraocular injections of VEGF-A (Peprotech), Flt-1 neutralizing antibody (R&D Systems), GFP- or Cre-expressing adenovirus (University of Iowa, Gene Transfer Vector Core) were conducted as described previously (Gerhardt et al., 2003). Briefly, WT (VEGF-A injections) and *flt-1*$^{+/-}$ (neutralizing antibody injections) mouse pups (P5) were anesthetized, and approximately 0.5 μl (1 μg/μl) of VEGF-A165, Flt-1 neutralizing antibody, or PBS was injected with a 10 μl Hamilton syringe. Injected mice were sacrificed after 6 hours, and retinas were perfusion-fixed with 0.5% PFA/PBS, harvested, and fixed for 2 hours with 2% PFA. *Flt-1*$^{flox/flox}$ (Genentech) and *flt-1*$^{flox/+}$ mouse pups (P3) were anesthetized, and approximately 0.5 μl (1×10^{10} PFU/ml) of GFP- or Cre-expressing adenovirus was injected into each eye. After 3-4 days, animals were sacrificed, and their retinas were harvested and fixed as described above. Retinal expression of genes delivered via adenovirus was confirmed by RT-PCR of infected retinas (data not shown).

Antibody Staining and Quantitative Analysis

Day 8 ES cell cultures were fixed and processed for antibody staining as described (Kappas et al., 2008). Primary antibodies used were: rat anti-mouse PECAM-1 (BD Biosciences) at 1:1000, goat (MP Biomedical) or rabbit (Invitrogen) polyclonal anti-β-galactosidase at 1:300, and goat anti-mouse Flt-1 (R&D Systems) at 1:300. Secondary antibodies were donkey anti-rat IgG (IgG; H+L) Rhodamine Red at 1:300 (Jackson ImmunoResearch), goat ant-rat IgG AlexaFluor488 (IgG; H+L) at 1:300 (Invitrogen), donkey anti-goat IgG AlexaFluor488 or AlexaFluor568 (IgG; H+L) at 1:300 (Invitrogen) and donkey anti-rabbit IgG AlexaFluor568 (IgG: H+L) at 1:300 (Invitrogen). Following staining, cultures were incubated with DAPI (1:1000) for 30 min. Imaging was with a confocal microscope (Leica TCS SP5) using a 40× objective (HCX PL APO oil). 8-10 z-axis confocal images were acquired, combined, and flattened.

Sprouting vessels in each culture were randomly selected for analysis of guidance parameters (Supp. Fig. 1). For sprout angles, the acute angle between the parent vessel axis and the sprouting vessel axis was measured. For distance measurements, tangents were extended from the sprout midpoint perpendicular to the sprout axis, and distance to the closest vessel measured. With 0° at the sprout leading edge and 180° at the sprout base, the filopodium angle was measured.

Retinas were fixed and processed for staining with isolectin GS-IB4 conjugated to AlexaFluor488 (Molecular Probes) as described (Gerhardt et al, 2003; Hellstrom et al., 2007). WT and *flt-1*$^{+/-}$ mouse retinas used in Flt-1 expression analysis were further stained with either a mouse monoclonal antibody to Flt-1 (Abcam) at 1:100 or rabbit polyclonal anti-β-galactosidase (Invitrogen) at 1:100, respectively. Secondary antibodies used in retinas were donkey anti-mouse IgG DyLight568 (IgG; H+L) at 1:300 (Jackson ImmunoResearch) and donkey anti-rabbit IgG DyLight568 (IgG; H+L) at 1:300 (Jackson ImmunoResearch). Retinas were imaged using a confocal microscope (LSM 5 Pascal, Carl Zeiss Inc.) and a 40× Plan-Neofluor oil objective (Carl Zeiss Inc.) as described for ES cell cultures. Retinal measurements included sprout distance but not sprout angle, because parent vessels could not be clearly identified at the vascular front.

Intensity of β-galactosidase staining in ES cell-derived and retinal vessels was assessed by outlining the sprout and adjacent base cells and measuring the mean intensity of the signal normalized to the area. All measurements were acquired with Image J software (NIH).

Live Imaging and Quantitative Analysis

Time-lapse imaging of day 7-8 ES cell cultures was performed as described previously (Kearney et al., 2004). Confocal images were acquired at 1 min intervals using Metamorph software (Universal Imaging Corp) and a CCD camera (Hamamatsu Orca) with a 20× objective. The rate of angle change was measured and quantified as follows: the angle of each sprout was measured every ten frames (i.e. in 10 minute intervals) by determining the angle between the sprout axis and the axis of the parent vessel; the change in sprout angle per 10 frames (10 min) was calculated for each interval and divided by 10, yielding a “degrees per minute” result. The degrees per minute values were averaged for the duration of the sprouting event

Statistics

Statistical significance in average rate of change in sprout angle and average number of filopodia per sprout length was determined using the Student's two-tailed t test. β-galactosidase expression ratios were statistically analyzed using the independent one-sample *t*-test where the null hypothesis was 1.0. All other values were statistically compared using χ^2 analysis.

Supplementary Material

Refer to Web version on PubMed Central for supplementary material.

Acknowledgments

We thank Rebecca Rapoport for technical support, Joe Kearney and Nick Kappas for help with live imaging, Joan Taylor for help with virus experiments, and Samantha Strickland for help with expression analysis. We thank Bob Goldstein, Suk-Won Jin, Mark Majesky, and Cam Patterson for critical comments on the manuscript, and Greg Matera for the use of his confocal microscope. This work was supported by NIH grants HL43174 and HL86564 to V.L.B., Fellowship support from the NIH (T32CA9156 and F32HL95359) and AHA (0826082E) to J.C.C., and Fellowship support from the NIH (T32HD46369) and AHA (0715187U) to S.M.T.

References

Carmeliet P, Ferreira V, Breier G, Pollefeyt S, Kieckens L, Gertsenstein M, Fahrig M, Vandenhoeck A, Harpal K, Eberhardt C, et al. Abnormal blood vessel development and lethality in embryos lacking a single VEGF allele. Nature 1996;380:435–439. [PubMed: 8602241]

Coultas L, Chawengsaksophak K, Rossant J. Endothelial cells and VEGF in vascular development. Nature 2005;438:937–945. [PubMed: 16355211]

Czirok A, Zamir E, Szabo A, Little C. Multicellular sprouting during vasculogenesis. Curr Topic Dev Biol 2008;81:269–289.

Damert A, Miquerol L, Gertsenstein M, Risau W, Nagy A. Insufficient VEGFA activity in yolk sac endoderm compromises haematopoietic and endothelial differentiation. Development 2002;129:1881–1892. [PubMed: 11934854]

Dorrell MI, Aguilar E, Friedlander M. Retinal vascular development is mediated by endothelial filopodia, a preexisting astrocytic template and specific R-Cadherin adhesion. Invest Ophthalmol Vis Sci 2002;43:3500–3510. [PubMed: 12407162]

Eichmann A, Yuan L, Moyon D, le Noble F, Pardanaud L, Breant C. Vascular development: from precursor cells to branched arterial and venous networks. Int J Dev Biol 2005;49:259–267. [PubMed: 15906240]

Ferrara N, Carver-Moore K, Chen H, Dowd M, Lu L, O'Shea KS, Powell-Braxton L, Hillan KJ, Moore MW. Heterozygous embryonic lethality induced by targeted inactivation of the VEGF gene. Nature 1996;380:439–442. [PubMed: 8602242]

Fong GH, Rossant J, Gertsenstein M, Breitman ML. Role of the Flt-1 receptor tyrosine kinase in regulating the assembly of vascular endothelium. Nature 1995;376:66–70. [PubMed: 7596436]

Fruttiger M. Development of the mouse retinal vasculature: angiogenesis versus vasculogenesis. Invest Ophthalmol Vis Sci 2002;43:522–527. [PubMed: 11818400]

Gerhardt H, Golding M, Fruttiger M, Ruhrberg C, Lundkvist A, Abramsson A, Jeltsch M, Mitchell C, Alitalo K, Shima D, et al. VEGF guides angiogenic sprouting utilizing endothelial tip cell filopodia. J Cell Biol 2003;161:1163–1177. [PubMed: 12810700]

Gerhardt H. VEGF and endothelial guidance in angiogenic sprouting. Organogenesis 2008;4:241–246. [PubMed: 19337404]

Hellstrom M, Phng LK, Hofmann JJ, Wallgard E, Coultas L, Lindbrom P, Alva J, Nilsson AK, Karlsson L, Gaiano N, et al. Dll4 signalling through Notch 1 regulates formation of tip cells during angiogenesis. Nature 2007;445:776–780. [PubMed: 17259973]

Holderfield MT, Hughes CCW. Crosstalk between vascular endothelial growth factor, notch, and transforming growth factor-β in vascular morphogenesis. Circ Res 2008;102:637–652. [PubMed: 18369162]

Horowitz A, Simons M. Branching morphogenesis. Circ Res 2008;103:784–795. [PubMed: 18845818]

Jakobsson L, Kreuger J, Claesson-Welsh L. Building blood vessels--stem cell models in vascular biology. J Cell Biol 2007;177:751–755. [PubMed: 17535968]

Jinnin M, Medici D, Park L, Limaye N, Liu Y, Boscolo E, Bischoff J, Vikkula M, Boye E, Olsen BR. Suppressed NFAT-dependent VEGFR1 expression and constitutive VEGFR2 signaling in infantile hemangioma. Nat Med 2008;14:1236–1246. [PubMed: 18931684]

Kappas NC, Zeng G, Chappell J, Kearney JB, Hazarika S, Kallianos K, Patterson C, Annex B, Bautch VL. The VEGF receptor Flt-1 spatially modulates Flk-1 signaling and blood vessel branching. J Cell Biol 2008;181:847–858. [PubMed: 18504303]

Kearney JB, Ambler CA, Monaco KA, Johnson N, Rapoport RG, Bautch VL. Vascular endothelial growth factor receptor Flt-1 negatively regulates developmental blood vessel formation by modulating endothelial cell division. Blood 2002;99:2397–2407. [PubMed: 11895772]

Kearney JB, Bautch VL. In vitro differentiation of mouse ES cells: hematopoietic and vascular development. Methods Enzymol 2003;365:83–98. [PubMed: 14696339]

Kearney JB, Kappas NC, Ellerstrom C, DiPaola FW, Bautch VL. The VEGF receptor flt-1 (VEGFR-1) is a positive modulator of vascular sprout formation and branching morphogenesis. Blood 2004;103:4527–4535. [PubMed: 14982871]

Keller G. Embryonic stem cell differentiation: emergence of a new era in biology and medicine. Genes Dev 2005;19:1129–1155. [PubMed: 15905405]

Kendall RL, Thomas KA. Inhibition of vascular endothelial cell growth factor activity by an endogenously encoded soluble receptor. Proc Natl Acad Sci USA 1993;90:10705–10709. [PubMed: 8248162]

Kowanetz M, Ferrara N. Vascular endothelial growth factor signaling pathways: Therapeutic Perspective. Clin Cancer Res 2006;12:5018–5022. [PubMed: 16951216]

Larina IV, Shen W, Kelly OG, Hadjantonakis AK, Baron MH, Dickinson ME. A membrane associated mCherry Fluorescent reporter line for studying vascular remodeling and cardiac function during muring embryonic development. Anat Rec 2009;292:333–341.

Li, X.; ClaessonWelsh, L.; Shibuya, M. In Meth Enzymol. Academic Press; 2008. VEGF receptor signal transduction; p. 261-284.

Lu P, Werb Z. Patterning mechanisms of branched organs. Science 2008;322:1506–1509. [PubMed: 19056977]

Mazzone M, Dettori D, Leite de Oliveira R, Loges S, Schmidt T, Jonckx B, Tian YM, Lanahan AA, Pollard P, Ruiz de Almodovar C, et al. Heterozygous deficiency of PHD2 restores tumor oxygenation and inhibits metastasis via endothelial normalization. Cell 2009;136:839–851. [PubMed: 19217150]

Risau W. Mechanisms of angiogenesis. Nature 1997;386:671–674. [PubMed: 9109485]

Roberts DM, Kearney JB, Johnson JH, Rosenberg MP, Kumar R, Bautch VL. The vascular endothelial growth factor (VEGF) receptor Flt-1 (VEGFR-1) modulates Flk-1 (VEGFR-2) signaling during blood vessel formation. Am J Pathol 2004;164:1531–1535. [PubMed: 15111299]

Roca C, Adams RH. Regulation of vascular morphogenesis by Notch signaling. Genes Dev 2007;21:2511–2524. [PubMed: 17938237]

Ruhrberg C, Gerhardt H, Golding M, Watson R, Ioannidou S, Fujisawa H, Betsholtz C, Shima DT. Spatially restricted patterning cues provided by heparin-binding VEGF-A control blood vessel branching morphogenesis. Genes Dev 2002;16:2684–2698. [PubMed: 12381667]

Shalaby F, Rossant J, Yamaguchi TP, Gertsenstein M, Wu XF, Breitman ML, Schuh AC. Failure of blood-island formation and vasculogenesis in Flk-1-deficient mice. Nature 1995;376:62–66. [PubMed: 7596435]

Shawber CJ, Funahashi Y, Francisco E, Vorontchikhina M, Kitamura Y, Stowell SA, Borisenko V, Feirt N, Podgrabinska S, Shiraishi K, et al. Notch alters VEGF responsiveness in human and murine endothelial cells by direct regulation of VEGFR-3 expression. J Clin Invest 2007;117:3369–3382. [PubMed: 17948123]

Stalmans I, Ng YS, Rohan R, Fruttiger M, Bouche A, Yuce A, Fujisawa H, Hermans B, Shani M, Jansen S, et al. Arteriolar and venular patterning in retinas of mice selectively expressing VEGF isoforms. J Clin Invest 2002;109:327–336. [PubMed: 11827992]

Suchting S, Freitas C, le Noble F, Benedito R, Breant C, Duarte A, Eichmann A. The Notch ligand Delta-like 4 negatively regulates endothelial tip cell formation and vessel branching. Proc Natl Acad Sci USA 2007;104:3225–3230. [PubMed: 17296941]

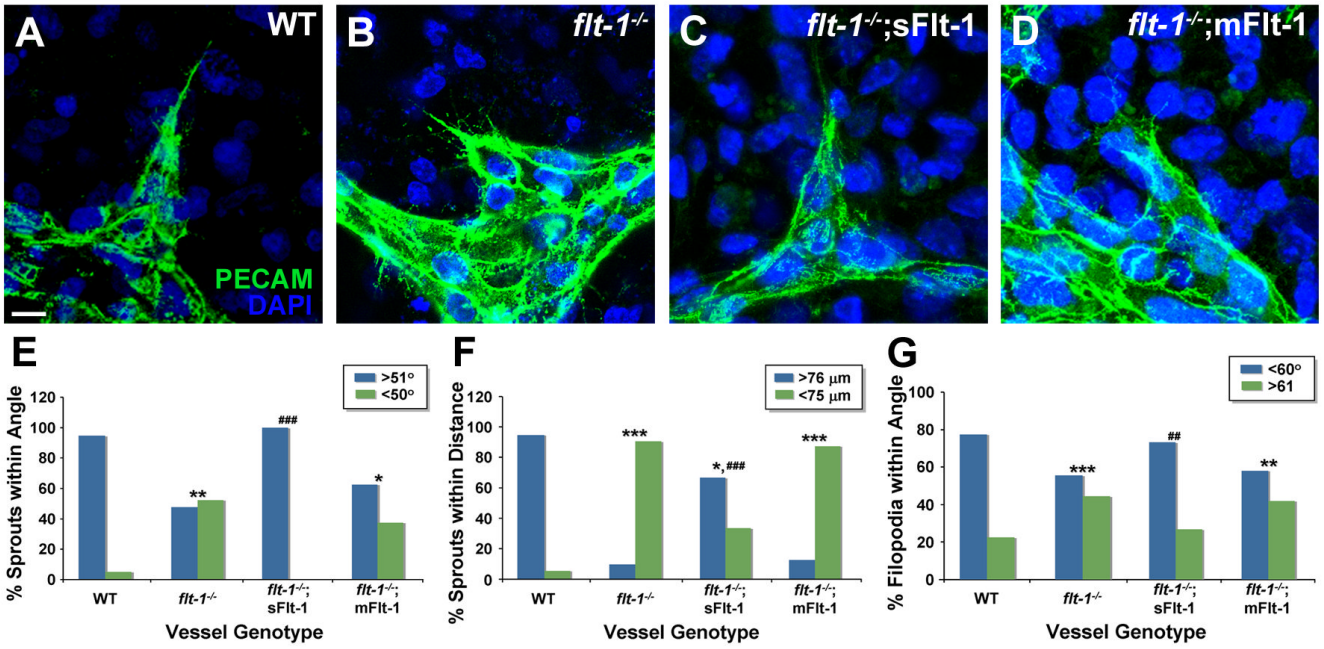

Figure 1. Vessel sprout guidance is perturbed by loss of soluble Flt-1 in ES cell-derived vessels

(A-D) Day 8 cultures were stained for PECAM-1 (green) and DAPI (nuclear, blue). Scale bar, 10 μm. (E-G) Vascular sprouts were assessed for guidance parameters, including sprout angle (E), distance between sprouts and existing vessels (F), and filopodia angle (G). In each graph, comparisons to WT are denoted: * = p≤0.04; ** = p≤0.002; *** = p≤0.0001; and comparisons to *flt-1*$^{-/-}$ are denoted: ## = p≤0.002; ### = p≤0.0008.

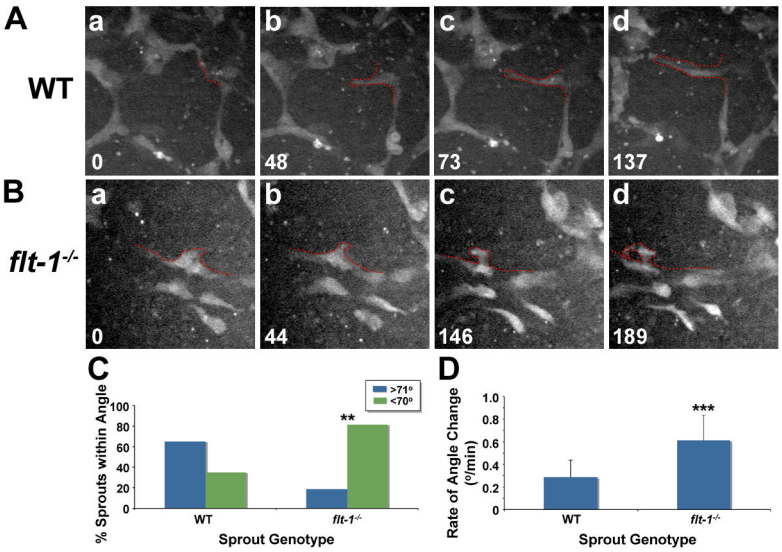

Figure 2. *Flt-1* mutant sprouts have a dynamic misguidance phenotype

(A-B) WT and *flt-1*$^{-/-}$ ES cell-derived vessels with PECAM-driven eGFP expression were visualized in real-time by spinning disc confocal microscopy. In each frame, time (min) is in lower left, and the sprouting vessel is outlined in red. (C-D) Time-lapse images of sprouting were analyzed for sprout angle (C: ** = $p \leq 0.006$) and the rate of sprout angle change over time (D: *** = $p \leq 0.0001$). (D) Values are averages + SD.

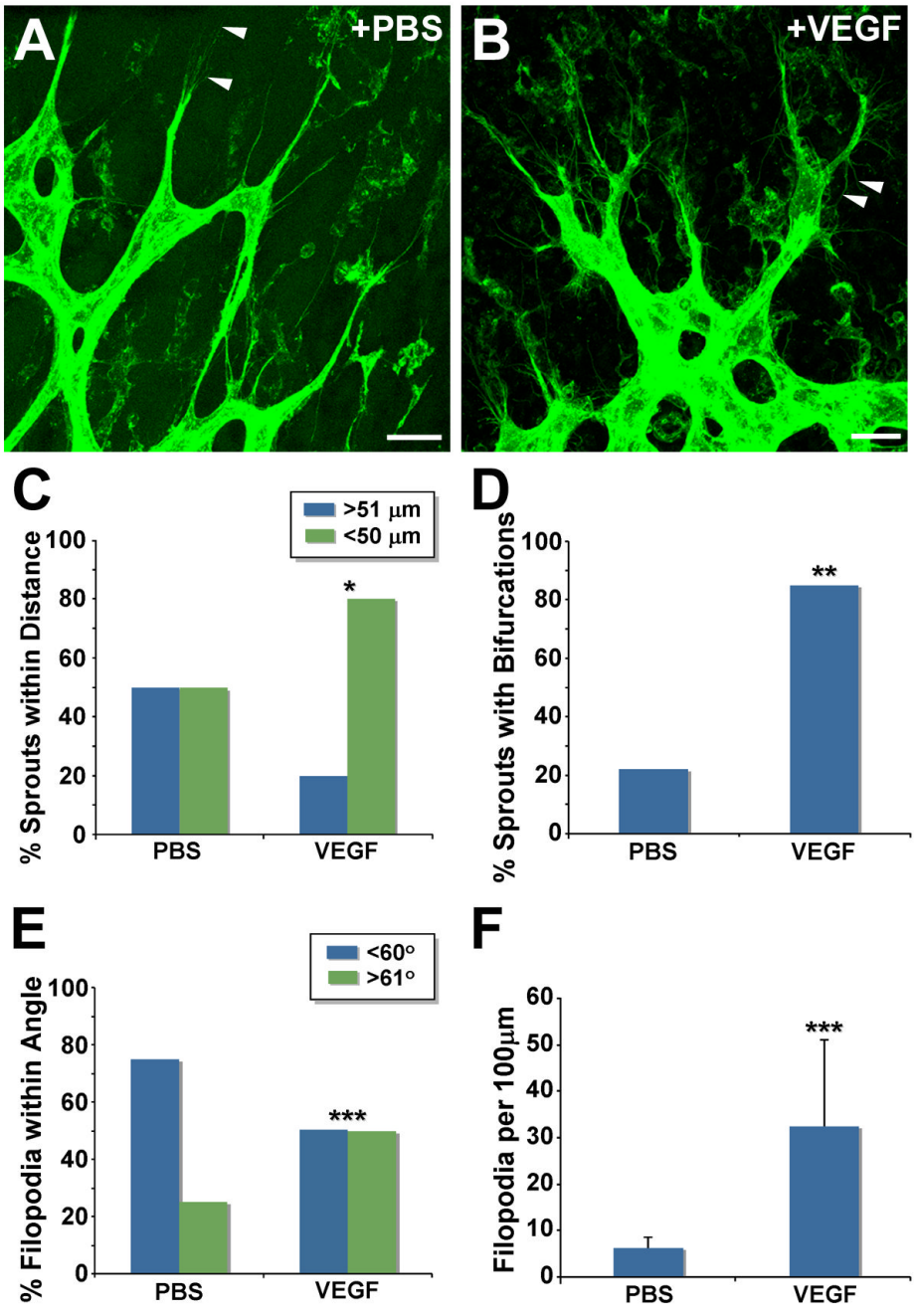

Figure 3. Exogenous VEGF-A disrupts local guidance of sprouting retinal vessels

(A-B) Confocal images of blood vessels from PBS- or VEGF-injected P5 mouse retinas stained with Alexa488-conjugated isolectin-B4. Arrowheads denote filopodia extended either in the direction of migration (A), or toward the sprout base (B). Scale Bar, 20 μm. (C-F) Vessel sprouts were analyzed for guidance parameters (C: * = $p \leq 0.05$; D: ** = $p \leq 0.001$; E and F: *** = $p \leq 0.0001$). (F) Values are averages + SD.

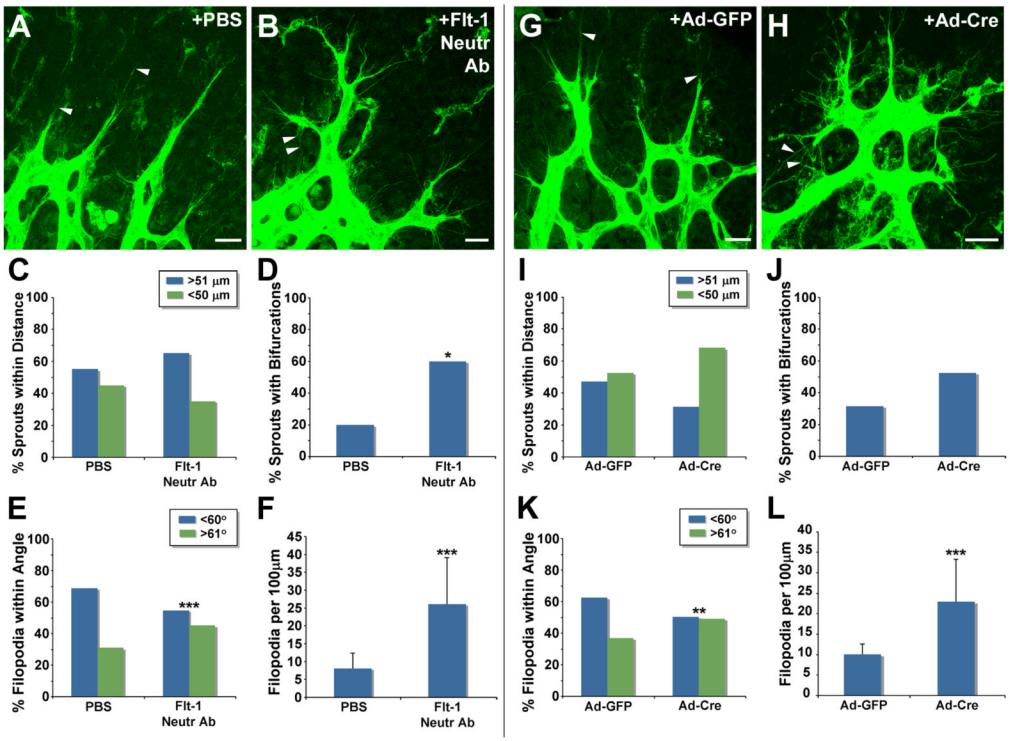

Figure 4. Loss of *flt-1* function disrupts local guidance of sprouting retinal vessels

(A-B) Confocal images of blood vessels from PBS- or Flt-1 neutralizing antibody-injected P5 mouse retinas stained with Alexa488-conjugated isolectin-B4. Arrowheads denote filopodia extended either in the direction of migration (A), or toward the sprout base (B). (C-F) Vessel sprouts were analyzed for guidance parameters (D: * = $p \leq 0.01$; E and F: *** = $p \leq 0.0002$). (F) Values are averages + SD. (G-H) Confocal images of blood vessels from P6 mouse retinas injected with adenovirus expressing either GFP (Ad-GFP) or cre-recombinase (Ad-Cre) on P3, and stained with Alexa488-conjugated isolectin-B4. Arrowheads denote filopodia extended either in the direction of migration (G), or toward the sprout base (H). (I-L) Vessel sprouts were analyzed for guidance parameters (K: ** = $p \leq 0.002$; L: *** = $p \leq 0.0001$). (L) Values are averages + SD. Scale Bar, 20 μm.

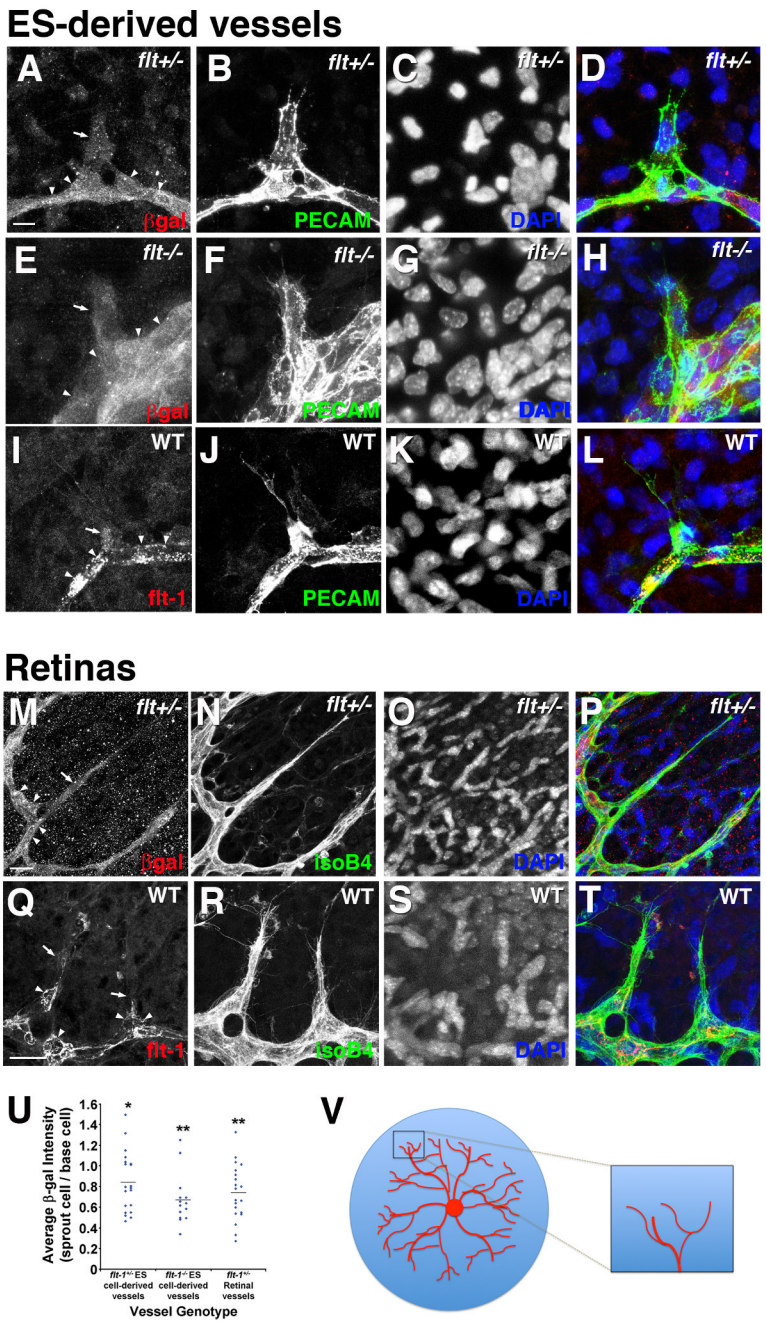

Figure 5. Flt-1 expression is enhanced in lateral base areas of sprouting vessels

(A-L), *flt-1*$^{+/-}$ (A-D) and *flt-1*$^{-/-}$ (E-H) ES cells cultured for 8 days were stained for β-galactosidase (red), PECAM-1 (green), and DAPI (nuclear, blue). (I-L) Day 8 WT cultures were stained for flt-1 (red), PECAM-1 (green), and DAPI (nuclear, blue). Arrows point to sprouts with lower β-galactosidase or Flt-1 reactivity, and arrowheads indicate base areas with higher β-galactosidase or Flt-1 reactivity. Scale bar, 10 μm. (M-T), P5 *flt-1*$^{+/-}$ mouse retinas (M-P) were stained with β-galactosidase (red), Alexa488-conjugated isolectin-B4 (green), and DAPI (nuclear, blue), and WT retinas (Q-T) were labeled for Flt-1 (red) instead of β-galactosidase. Scale bar, 20 μm. Arrows point to sprouts with lower β-galactosidase or Flt-1 reactivity, and arrowheads indicate base cells with higher β-galactosidase or Flt-1 reactivity.

(U) Ratio of β-galactosidase expression in the sprout cells relative to each lateral base cell for randomly selected sprouting vessels in *flt-1*$^{+/-}$ and *flt-1*$^{-/-}$ ES-derived vessels and *flt-1*$^{+/-}$ retinal vessels. Blue diamonds represent individual sprout/lateral base ratios, and the black horizontal lines are the mean for each group. β-galactosidase expression ratios were statistically analyzed using the independent one-sample *t*-test where the null hypothesis was 1.0 (* = $p \leq 0.02$; ** = $p \leq 0.001$). (V) Schematic of retinal vasculature in the developing mouse eye. The boxed area is the area of the retina shown in panels M-T.

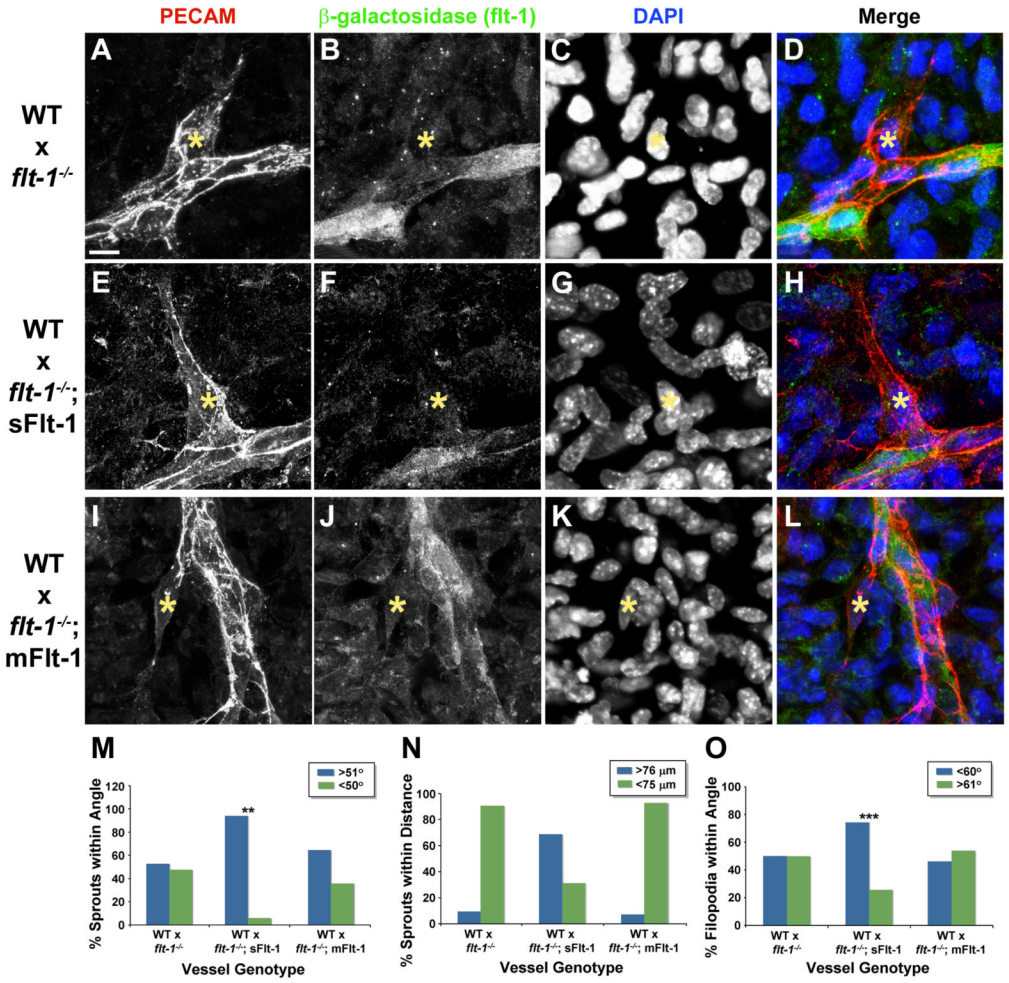

Figure 6. Local sprout guidance requires sFlt-1 in lateral base areas

Mosaic vessels composed of WT ES cells mixed with either *flt-1*$^{-/-}$ (A-D), *flt-1*$^{-/-}$;sFlt-1 (E-H), or *flt-1*$^{-/-}$;mFlt-1 (I-L) ES cells were cultured 8 days, then labeled with antibodies for PECAM-1 (red), β-galactosidase (green), and DAPI (nuclear dye, blue). Scale bar, 10 μm. Mosaic vessels were assessed for sprout angle (M: WT:*flt-1*$^{-/-}$ vs. WT:*flt-1*$^{-/-}$;sFlt, ** = p≤0.007), distance between sprout and existing vessel (N), and filopodia angle (O: WT:*flt-1*$^{-/-}$ vs. WT:*flt-1*$^{-/-}$;sFlt, *** = p≤0.0001).

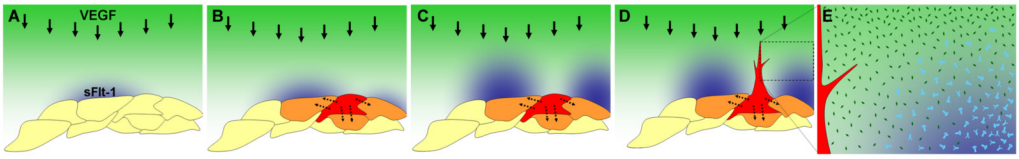

Figure 7. Model for sFlt-1 regulation of vessel sprout guidance

The schematic model illustrates how expression of sFlt-1 (blue; light blue "Y"s in E) in lateral base areas might regulate local sprout guidance by reducing the concentration of free VEGF (green; dark green diamonds in E) in regions adjacent to the emerging sprout (red). Dotted lines show potential endothelial cross-talk to reinforce heterogeneity. (A-D), changes with time, (E) blow-up of box in D showing how local sFlt-1 might neutralize VEGF-A (light blue diamonds) to provide a "corridor" for sprout emergence.